Islamic Azad University

Journal of

Optoelectronical Nanostructures

Autumn 2019 / Vol. 4, No. 4

Ultra-Compact Bidirectional Terahertz Switch Based on Resonance in Graphene Ring and Plate

Mehdi Dehghan[1], Mohammad Kazem Moravvej-Farshi[2], Mohsen Ghaffari-Miab[2], Masoud Jabbari[*,3], Ghafar Darvish[1]

[1] Department of Electrical Engineering, Science and Research Branch, Islamic Azad University, Tehran 1477893855, Iran.
[2] Faculty of Electrical and Computer Engineering, The Nano Plasmo-Photonic Research group, Tarbiat Modares University, Tehran 1411713116, Iran.
[3] Department of Electrical Engineering, Marvdasht Branch, Islamic Azad University, Marvdasht, Iran.

(Received 14 Jun. 2019; Revised 23 Jul. 2019; Accepted 11 Aug. 2019; Published 15 Sep. 2019)

Abstract: In this paper, we present a switch based on coupling and resonance in the graphene plate and rings operating at 10 THz. This structure consists of several layers of Hexagonal Boron Nitride (hBN), SiO2 and P^+Si, such that graphene plates and rings are inside the hBN layer. The terahertz wave is incident from the upper part of the switch and Surface Plasmons (SPs) are excited by the grating in the structure on the graphene plate beneath the nano-aperture and moves towards the ports available on the left and right of the switch. At first, at the certain applied voltage, the SPs cross the left port and this port is ON. With the increase in voltage and the change in the chemical potential, switching occurs and the SPs exit from the right and this port is ON while the left port turns OFF. The extinction ratio in this structure is 18dB and the size of the structure is 1μm. Aforementioned benefits make this switch the best choice for using in integrated optical circuits.

Keywords: Bidirectional Switch, Graphene, Resonance, Chemical Potential

1. INTRODUCTION

Terahertz technology has been used for its unique potential in a variety of applications, including high-speed communication. Corresponding to the development of resources in the terahertz frequency domain [1–5] as well as terahertz detectors [6–9], devices operating in this frequency range, including modulators [10–12], filters [13–15] and switches [16–18], have been widely considered and developed. On the other hand, plasmonics, as a bridge between electronics and photonics, reduce the dimensions below the wavelength. In

* Corresponding author. Email: **masoudjabbari@yahoo.com**

terahertz frequency, metal acts as a perfect electric conductor and this is one of the crucial problems since it causes an increase in loss. By using graphene we can overcome such problems. Graphene, as a two-dimensional material with a hexagonal structure, has special electrical, mechanical and thermal properties [19–21]. One thing that can increase the graphene's special properties is to place it on a similar structure as hBN [22]. Various structures have been proposed for optical switches up to now. However, the design of a bidirectional switch in the terahertz frequency with small size and high extinction ratio is considered in this article. COMSOL software has been used in this paper in order to simulation and analysis of transmittance in the proposed structure.

2. EFFECTIVE REFRACTIVE INDEX

The electrical conductivity of graphene can be restored using the Kubo formula [23–25]

$$\sigma_{\text{intra}} = \frac{ie^2 k_B T}{\pi\hbar^2(\omega + i\Gamma)}\left[\frac{\mu_c}{k_B T} + 2\ln\left(e^{-\frac{\mu_c}{k_B T}} + 1\right)\right] \tag{1}$$

$$\sigma_{\text{inter}} = \frac{ie^2}{4\pi\hbar}\ln\left[\frac{2\mu_c - (\omega + i\Gamma)\hbar}{2\mu_c + (\omega + i\Gamma)\hbar}\right] \tag{2}$$

$$\sigma = \sigma_{\text{intra}} + \sigma_{\text{inter}} \tag{3}$$

where e is the electron charge, k_B is the Boltzman constant, $\hbar$ is the reduced Plank constant, μ_c is the chemical potential, Γ=1.67THz is the scattering rate. Besides, by applying external voltage to the graphene, its chemical potential can be changed as follows [26].

$$|\mu_C| \approx \hbar v_F \sqrt{\pi a_0 |V - V_{\text{Dirac}}|} \tag{4}$$

where, the V_{Dirac}= 0.8 V is the offset voltage, v_f= 9×10^5, Fermi velocity and a_0= 9×10^{16} $m^{-2}V^{-1}$ constant for the parallel plate capacitance. Accordingly, by having graphene thickness Δ and graphene electrical conductivity, graphene permittivity can be calculated as the following equation [27–28]

$$\varepsilon_g = 1 - \frac{\text{Im}(\sigma)}{\omega\varepsilon_0\Delta} + i\frac{\text{Re}(\sigma)}{\omega\varepsilon_0\Delta} \tag{5}$$

On the other hand, the dispersion relation in the waveguide is calculated by [29]

$$-\frac{\gamma_1\varepsilon_{r2}}{\gamma_2\varepsilon_{r1}}=\left(1+\frac{i\sigma_g\gamma_1}{\omega\varepsilon_{r1}\varepsilon_0}\right)\tanh(\gamma_2 d)\ ,\ \gamma_1=k_0\sqrt{n_{\text{eff}}^2-\varepsilon_{r1}}\ ,\ \gamma_2=k_0\sqrt{n_{\text{eff}}^2-\varepsilon_{r2}} \qquad (6)$$

where, d is the distance between the metal and the graphene plate, γ_1 and γ_2 are the attenuation coefficients, in which k_0 is the free space wave number, and $n_{\text{eff}}=\beta/k_0$ and β are the SPs effective mode index and propagation constant. Considering the relation given for the graphene electrical conductivity, the real and imaginary part of the graphene surface conductivity versus frequency and in different chemical potentials is shown in Fig. 1 (a) and (b). Surface conductivity in this figure is normalized with $\sigma_0=e^2/(\pi\hbar)$.

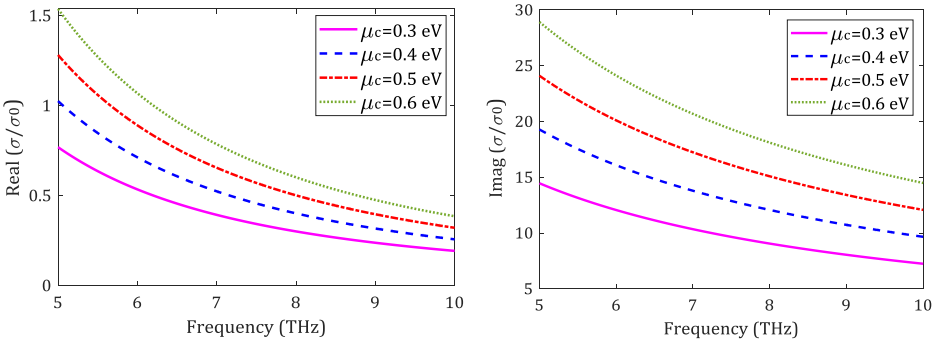

(a) (b)

Fig. 1 Real and imaginary parts of the normalized optical conductivity of graphene versus frequency for different chemical potential.

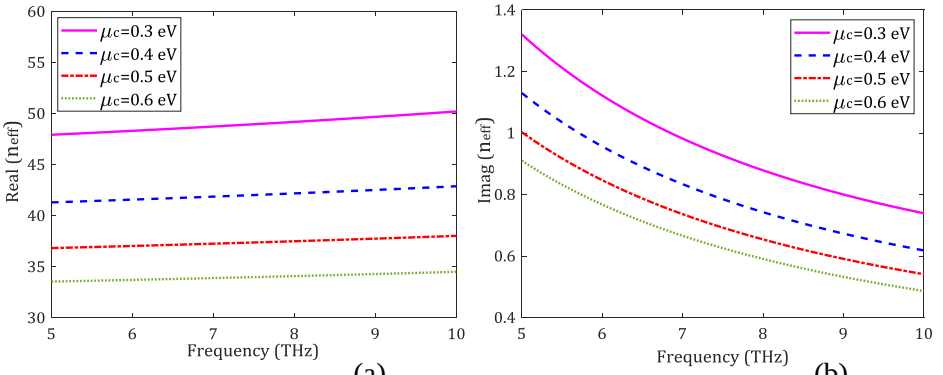

(a) (b)

Fig. 2 The real part and (b) the imaginary part of the effective refractive index for the structure

Using the dispersion relation and having the graphene electrical conductivity, the real and imaginary part of the effective refractive index of the structure is shown in Fig. 2 (a) and (b). As can be seen in this figure, the real and imaginary part decreases with increasing the chemical potential.

3. TRANSMITTANCE IN SIMPLE WAVEGUIDE

To investigate the resonance and to see how it changes with various parameters including the width of the graphene plates, the chemical potential and the distance between the graphene plates and ring we consider a simple waveguide shown in Fig. 3.

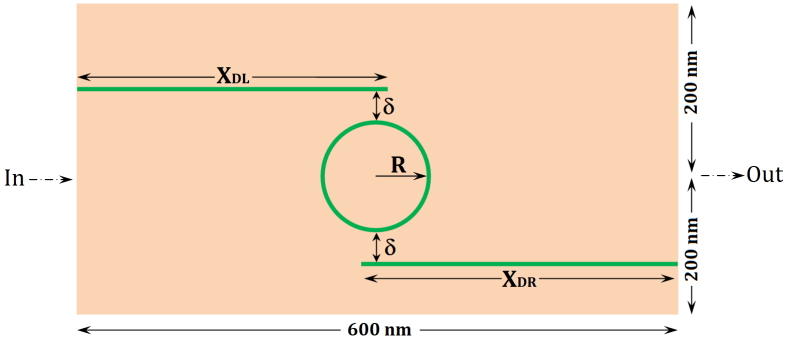

Fig. 3 a simple waveguide including graphene plates and ring in order to investigate the effect of overlap and resonance on transmittance

In this figure, a 600 nm×400 nm hBN waveguide is considered. In the middle of this structure, there is a graphene ring with the radius of *R* and two graphene plates with the width of X_{DL}= X_{DR}=330 nm which the distance between the ring and plates is δ. For this structure, the input port is on the left and the output port is on the right side. In this structure, the radius of the graphene ring is a determinant factor in resonance and by changing the radius of the graphene ring, the transmittance from the device is determined in the certain chemical potential. In Figure 4, the transmittance versus the radius of the graphene ring at 10 THz and for μ_c=0.3 eV is shown.

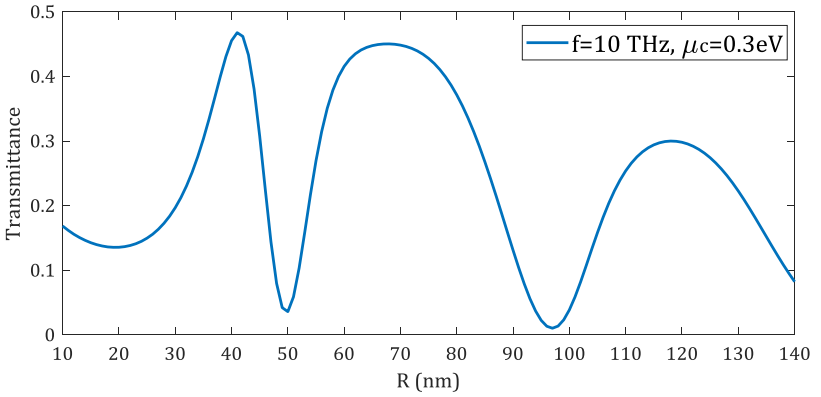

Fig. 4 The transmittance for the proposed structure at 10THz, μ_c=0.3 eV and $X_{DL}=X_{DR}$=330 nm.

As can be seen in this figure, for μ_c=0.3 eV and at 10THz the resonance occurred in R=40, 70, 120 nm. Now, with R=70 nm obtained from Fig. 4, the frequency spectrum of the transmittance for several chemical potentials is shown in Fig. 5.

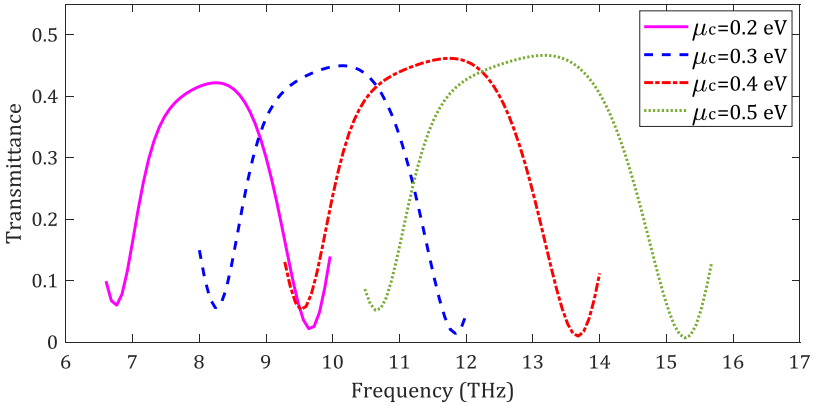

Fig. 5 Frequency spectrum of transmittance for proposed structure at different chemical potential and with R=70 nm and $X_{DL}=X_{DR}$=330 nm.

As can be observed from this figure, with increasing the chemical potential, the frequency spectrum of transmittance is shifted to the higher frequencies. In Fig. 6, the effect of distance between graphene plates and ring on the transmittance is shown for μ_c=0.3 eV, R=70nm and $X_{DL}= X_{DR}$=330 nm. As can be seen in this figure, the best distance between the graphene ring and plates is δ=20 nm which this amount will be used in designing the proposed switch structure.

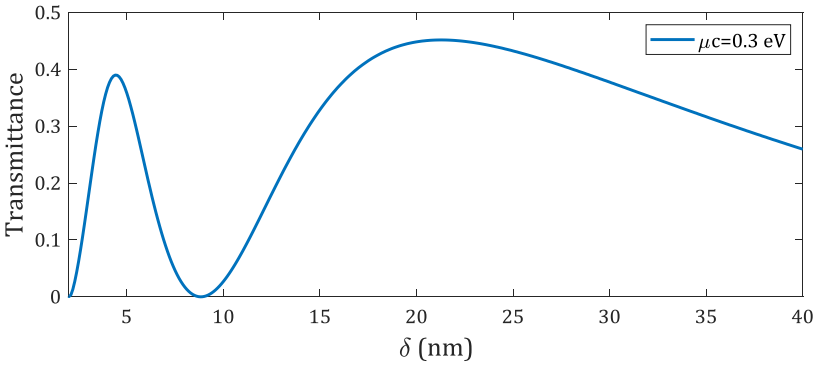

Fig. 6 Transmittance versus the distance of the graphene ring and plates for μ_c=0.3 eV, R=70 nm and X_{DL}=X_{DR}=330 nm.

4. BIDIRECTIONAL TERAHERTZ SWITCH

Now, by specifying the effect of different parameters in the transmittance, the main structure of the switch is presented. The proposed bidirectional terahertz switch structure is shown in Fig. 7.

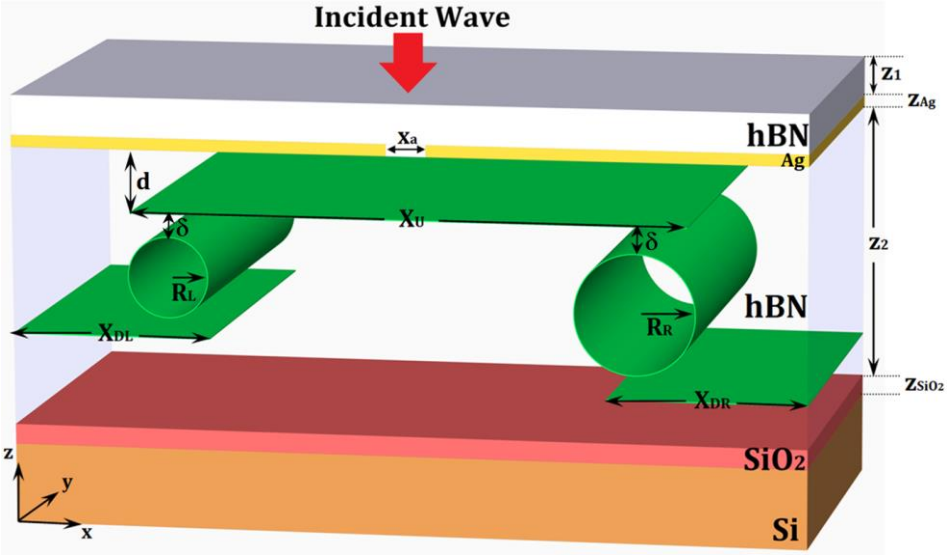

Fig 7. Bidirectional Terahertz Switch Structure

As shown in Fig. 7, in this structure, a SiO_2 layer with thickness Z_{SiO2}=50 nm is first placed on P^+Si. Then an hBN layer with thickness Z_2=450 nm is grown on it so that, graphene plates and rings are placed inside the hBN. Then Ag film

with Z_{Ag}=50 nm is placed on the top of hBN and 40nm nano-aperture is created in the middle of this layer and this nano-aperture plays the role of grating and excites SPs in the graphene layer beneath the gap. Finally, the hBN layer with Z_1=100 nm is placed on the top of the structure. This layer is placed to prevent reflection from the upper surface. For the thinner hBN layer the input impedance and reflection from the top of the device are increased and hence the transmittance is decreased. Given that the switching wavelength is 30μm and this wavelength is much larger in comparison with the dimensions of the structure, the excessive increase in the thickness of the top hBN layer does not affect the amount of output. Graphene rings on the left and right side of nano-aperture are asymmetric. As can be observed in Fig. 8 (a) and (b), in order to determine the best radius for R_R and R_L, these values have been changed simultaneously. Accordingly, the best performance of this switch occurred for R_R=115 nm and R_L=75 nm.

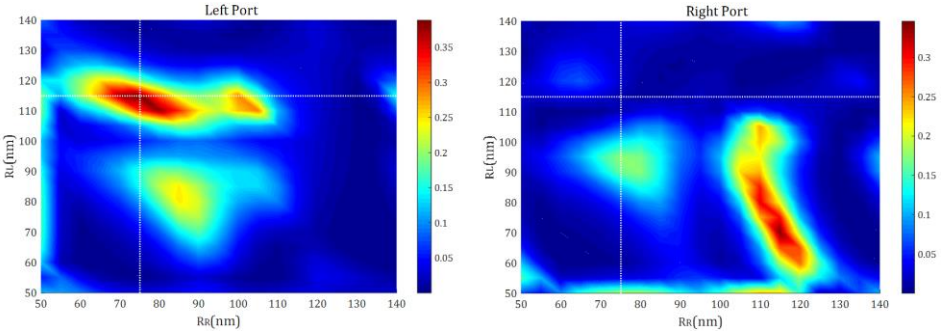

(a) (b)

Fig. 8 Transmittance versus R_R and R_L before switching at 10THz, X_{DL}=X_{DR}=330 nm, X_U=690 nm and δ=20 nm.

The width of the upper graphene plate is X_U= 690 nm and the width of the left and right graphene plates under the rings are the same and X_{DL}=X_{DR}=330 nm. Also according to Fig. 6 the distance between the graphene ring and plates is δ=20 nm. In this structure, the terahertz wave is incident from the top of the structure and due to the grating, the SPs are excited on the graphene plate beneath the nano-aperture and by making coupling and resonance in the graphene plates and rings they can be transferred to the ports on the left and right side of the nano-aperture. According to the (4), the distance between upper graphene plate and metal film *d* plays a significant role in the effective refractive index of the structure. If this distance is very small, the imaginary part of the effective refractive index of the structure will be very high and the loss increases, whereby the wave is not transmitted effectively. By increasing this distance more than a certain value, the effect of the field under the gap on the

bottom graphene plate is reduced and the SPs cannot be excited on this plate and thus, the transmittance is reduced. The width of the nano-aperture in the Ag film plays a crucial role in grating in the structure. If the width of the aperture is too small, the wave cannot enter the structure and with the excessive increase in the aperture width, this aperture cannot act as an efficient grating. Finally, the frequency spectrum transmitted from the switch before and after switching is shown in Fig. 9 (a) and (b), respectively. As can be seen from this figure, before switching and for applied voltage V=2.038 V which is equivalent to μ_c=0.45 eV wave travels from the left port and in fact, this port is ON, while the transmittance from the right port is negligible and this port is OFF. By increasing the applied voltage to V= 4.253 V which is equivalent to μ_c=0.65 eV, switching has occurred and the wave travels from the right and this port turns ON while the transmittance from the left port is negligible and this port is OFF.

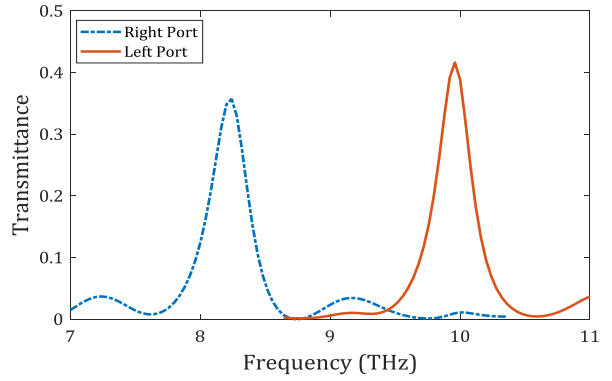

(a)

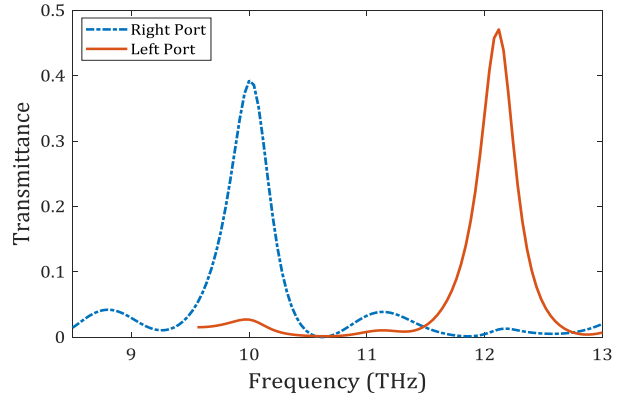

(b)

Fig. 9 Transmittance from the left and right ports for X_{DL}=X_{DR}=330 nm, X_U=690 nm, δ=20 nm and (a) before switching for μ_c=0.45 eV (b) after switching for μ_c=0.65 eV

Eventually, the profiles of the electric field at 10 THz before and after switching are shown in Fig. 10 (a) and (b), respectively.

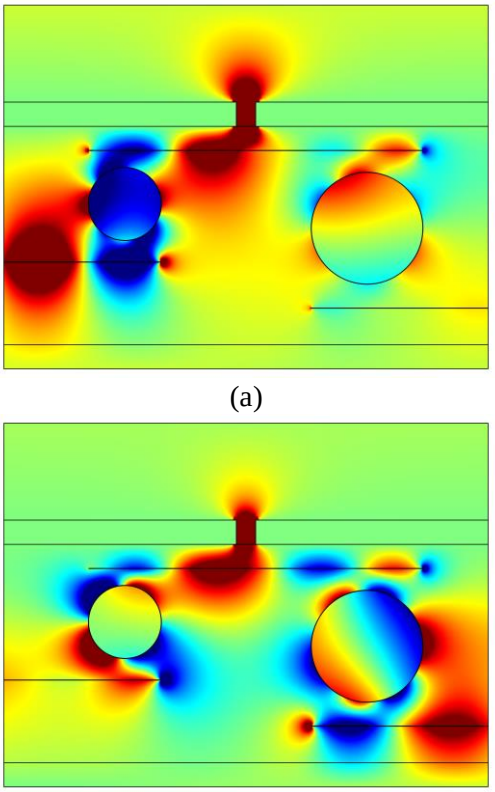

(a)

(b)

Fig. 10 Electric field profile at 10 THz for (a) before switching for μ_c=0.45 eV and (b) after switching for μ_c=0.65 eV

5. CONCLUSION

In this paper, a bidirectional terahertz switch structure based on coupling and resonance in graphene plates and rings is presented. Initially, a simple structure is presented to examine the effect of different parameters including graphene plate width, chemical potential and the space between the graphene plates and ring on the transmittance and resonance of a simple structure. In the final structure, the wave is incident from the top of the switch, and grating in this structure causes the SPs to excite on the graphene plate under the nano-aperture and the SPs can move toward the ports on the left and right sides of the

structure. Considering the input voltage of V=2.038 V which is equivalent to the chemical potential of μ_c=0.45 eV the left port is ON while the right port is OFF. By increasing Voltage to V=4.253 V which is equivalent to the chemical potential of μ_c=0.65 eV, switching occurs and the left port is OFF while the right port is ON. The amount of extinction ratio in this structure is 18dB. This extinction ratio, as well as ultra-compact dimensions, makes this structure a good choice for integrated optical circuits.

REFERENCES

[1] R. Kohler, A. Tredicucci, F. Beltram, H. E. Beere, E. H. Linfield, A. G. Davies, D. A. Ritchie, R. C. Iotti, and F. Rossi, *Terahertz semiconductor heterostructure laser*, Nature, 417 (2002) 156–159.
Available: https://www.nature.com/articles/417156a.

[2] R. W. Adams, K. Vijayraghavan, Q. J. Wang, J. Fan, F. Capasso, S. P. Khanna, A. G. Davies, E. H. Linfield, and M. A. Belkin, *GaAs/Al0.15Ga0.85 As terahertz quantum cascade lasers with doublephonon resonant depopulation operating up to 172 K*, Appl. Phys. Lett., 97 (131111) (2010).
Available: https://aip.scitation.org/doi/10.1063/1.3496035.

[3] M.A. Belkin, Q. J. Wang, C. Pflugl, A. Belyanin, S. P. Khanna, A. G. Davies, E. H. Linfield, and F. Capasso, *High-temperature operation of terahertz quantum cascade laser sources*, IEEE J. Select. Topics Quantum Electron., 15(3) (2009) 952–967.
Available: https://ieeexplore.ieee.org/document/4912319.

[4] Y. Chassagneux, Q. J. Wang, S. P. Khanna, E. Strupiechonski, J. R. Coudevylle, E. H. Linfield, A. G. Davies, F. Capasso, M. A. Belkin, and R. Colombelli, *Limiting factors to the temperature performance of THz quantum cascade lasers based on the resonant-phonon depopulation scheme*, IEEE Trans. Terahertz Sci. Technol., 2(1) (2012) 83–92.
Available: https://ieeexplore.ieee.org/document/6111503.

[5] G. Z. Liang, H. K. Liang, Y. Zhang, S. P. Khanna, L. H. Li, A. G. Davies, E. H. Linfield, D. F. Lim, C. S. Tan, S. F. Yu, H. C. Liu, and Q. J. Wang, *Single-mode surface-emitting concentric-circular-grating terahertz quantum cascade lasers*, Appl. Phys. Lett., 102 (031119) (2013).
Available: https://aip.scitation.org/doi/10.1063/1.4789535.

[6] S. Komiyama, O. Astafiev, V. Antonov, T. Kutsuwa, and H. Hirai, *A single-photon detector in the far-infrared range*, Nature, 403 (2000) 405–407,
Available: https://www.nature.com/articles/35000166.

[7] Denis A. Bandurin et al, *Resonant terahertz detection using graphene plasmons*, Nature Communications, 9(5392) (2018). Available: https://www.nature.com/articles/s41467-018-07848-w.

[8] A. Suziedelis, J. Gradauskas, S. Asmontas, G. Valusis, and H. G. Roskos , *Giga- and terahertz frequency band detector based on an asymmetrically necked n-n+ - GaAs planar structure*, Journal of Applied Physics, 93(5) (2003), Available: https://aip.scitation.org/doi/10.1063/1.1536024.

[9] Hamid Faezinia, Mahdi Zavvari, *Quantum modeling of light absorption in graphene based photo-transistors*, JOPN, 2(1) (2017) 9-20. Available: http://jopn.miau.ac.ir/article_2196.html.

[10] Hou-Tong Chen, Willie J. Padilla, Michael J. Cich, Abul K. Azad, Richard D. Averitt and Antoinette J. Taylor , *A metamaterial solid-state terahertz phase modulator*, Nature Photonics 3 (2009) 148-151. Available: https://www.nature.com/articles/nphoton.2009.3.

[11] Sheng Qu, Congcong Ma & Hongxia Liu, *Tunable graphene based hybrid plasmonic modulators for subwavelength confinement*, Scientific Reports, 7(5190) (2017). Available: https://www.nature.com/articles/s41598-017-05172-9.

[12] Baohu Huang, Weibing LU, Zhenguo Liu, and Siping Gao, *Low-energy high-speed plasmonic enhanced modulator using graphene*, Optics Express, 26(6) (2018) 7358-7367. Available: https://www.osapublishing.org/oe/abstract.cfm?URI=oe-26-6-7358.

[13] Jin Tao, Bin Hu, Xiao Yong He, and Qi Jie Wang, *Tunable Subwavelength Terahertz Plasmonic Stub Waveguide Filters*, IEEE Transaction on Nanotechnology, 12(6) (2013) 1191-1197. Available: https://ieeexplore.ieee.org/abstract/document/6626633.

[14] Bin Shi, Wei Cai, Xinzheng Zhang, Yinxiao Xiang, Yu Zhan, Juan Geng, Mengxin Ren and Jingjun Xu, *Tunable Band-Stop Filters for Graphene Plasmons Based on Periodically Modulated Graphene*, Scientific Reports, 6(26796) (2016), Available: https://www.nature.com/articles/srep26796.

[15] Hong-Ju Li, Ling-Ling Wang, Bin Sun, Zhen-Rong Huang, and Xiang Zhai, *Tunable mid-infrared plasmonic band-pass filter based on a single graphene sheet with cavities*, Journal of Applied Physics, 116(22) (2014) 224505, Available: https://aip.scitation.org/doi/full/10.1063/1.4903965.

[16] Mehdi Dehghan, Mohammad Kazem Moravvej-Farshi, Mohsen Ghaffari-Miab, Masoud Jabbari and Ghafar Darvish, *Ultra-compact Spatial*

Terahertz Switch Based on Graphene Plasmonic-Coupled Waveguide, Plasmonics, 1-11 (2019).
Available: https://link.springer.com/article/10.1007/s11468-019-00921-0.

[17] M. Ghorbanzadeh, S. Darbari, and M. K. Moravvej-Farshi, *Graphene-based plasmonic force switch*, Applied Physics Letters, 108(111105) (2016), Available: https://aip.scitation.org/doi/10.1063/1.4944332.

[18] Ognjen Ilic, Nathan H. Thomas, Thomas Christensen, Michelle C. Sherrott, Marin Soljačić,Austin J. Minnich, Owen D. Miller and Harry A. Atwater, *Active Radiative Thermal Switching with Graphene Plasmon Resonators*, ACS Nano, 12 (3) (2018) 2474–2481.
Available: https://pubs.acs.org/doi/10.1021/acsnano.7b08231.

[19] K. S. Novoselov, A. K. Geim, S. V. Morozov, D. Jiang, Y. Zhang, S. V. Dubonos, I. V. Grigorieva, A. A. Firsov, *Electric Field Effect in Atomically Thin Carbon Films*, Science, 306(5696) (2004) 666-669.
Available: https://science.sciencemag.org/content/306/5696/666.

[20] Qiaoliang Bao and Kian Ping Loh, *Graphene Photonics, Plasmonics, and Broadband Optoelectronic Devices*, ACS Nano, 6(5) (2012) 3677–3694.
Available: https://pubs.acs.org/doi/10.1021/nn300989g.

[21] Maryam Hojatifar, Peyman Sahebsara, *Tight- binding study of electronic band structure of anisotropic honeycomb lattice*, JOPN, 1(3) (2016) 17-26.
Available: http://jopn.miau.ac.ir/article_2190.html.

[22] D. Kaplan, G. Recine, and V. Swaminathan, *Electrically dependent bandgaps in graphene on hexagonal boron nitride*, Applied Physics Letters, 104(133108) (2014).
Available:
https://aip.scitation.org/doi/abs/10.1063/1.4870769?journalCode=apl.

[23] Hanson G.W., *Dyadic Green's functions and guided surface waves for a surface conductivity model of graphene*, J. Appl. Phys., 103, (6) (2008) 1–18, Available: https://aip.scitation.org/doi/full/10.1063/1.2891452.

[24] P.-Y. Chen and A. Al`u, *Atomically thin surface cloak using graphene monolayers*, ACS Nano, 5 (2011) 5855–5863.
Available: https://pubs.acs.org/doi/abs/10.1021/nn201622e.

[25] M. Liu, X. Yin, E. Ulin-Avila, B. Geng, T. Zentgraf, L. Ju, F. Wang, X. Zhang, *A graphene-based broadband optical modulator*, Nature 474 (2011) 64–67.
Available: https://www.nature.com/articles/nature10067.

[26] Hadi Rahimi, *Absorption Spectra of a Graphene Embedded One Dimensional Fibonacci Aperiodic Structure*, JOPN, 3(4) (2018) 45-58. Available: http://jopn.miau.ac.ir/article_3259.html.

[27] Zhu B., Ren G., Zheng S., Lin Z., Jian S., *Nanoscale dielectric-graphene-dielectric tunable infrared waveguide with ultrahigh refractive indices*, Opt. Express, 21 (14) (2013) 17089–17096. Available: https://www.osapublishing.org/oe/abstract.cfm?uri=oe-21-14-17089.

[28] Ooi K.J.A., Chu H.S., Ang L.K., Bai P., *Mid-infrared active graphene nanoribbon plasmonic waveguide devices*, J. Opt. Soc. Am. B, 30, (12), (2013) 3111. Available: https://www.osapublishing.org/josab/abstract.cfm?uri=josab-30-12-3111.

[29] X. Gu, I-T. Lin, J.-M. Liu, *Extremely confined terahertz surface plasmon-polaritons in graphene-metal structures*, Appl. Phys. Lett. 103 (7) (2013) 071103, Available: https://aip.scitation.org/doi/10.1063/1.4818660.